ACS OMEGA

http://pubs.acs.org/journal/acsodf

Article

Lipid-Dependent Titration of Glutamic Acid at a Bilayer Membrane Interface

Matthew J. McKay, Kelsey A. Marr, Jake R. Price, Denise V. Greathouse, and Roger E. Koeppe, II*

Cite This: *ACS Omega* 2021, 6, 8488–8494

Read Online

ACCESS | Metrics & More | Article Recommendations | Supporting Information

ABSTRACT: The ionization properties of protein side chains in lipid-bilayer membranes will differ from the canonical values of side chains exposed to an aqueous solution. While the propensities of positively charged side chains of His, Lys, and Arg to release a proton in lipid membranes have been rather well characterized, the propensity for a negatively charged Glu side chain to receive a proton and achieve the neutral state in a bilayer membrane has been less well characterized. Indeed, the ionization of the glutamic acid side chain has been predicted to depend on its depth of burial in a lipid membrane but has been difficult to verify experimentally. To address the issue, we incorporated an interfacial Glu residue at position 4 of a distinct 23-residue transmembrane helix and used ^{2}H NMR to examine the helix properties as a function of pH. We observe that the helix tilt and azimuthal rotation vary little with pH, but the extent of helix unraveling near residues 3 and 4 changes as the Glu residue E4 titrates. Remarkably, the ^{2}H quadrupolar splitting for the side chain of alanine A3 responds to pH with an apparent pK_a of 4.8 in 1,2-dilauroyl-*sn*-glycero-3-phosphocholine (DLPC) and 6.3 in 1,2-dimyristoyl-*sn*-glycero-3-phosphatidylcholine (DMPC), but is unchanged up to pH 8.0 in 1,2-dioleoyl-*sn*-glycero-3-phosphocholine (DOPC) in the presence of residue E4. With bilayers composed of alkali-stable ether-linked lipids, the side chain of A3 responds to pH with an apparent pK_a of 11.0 in the ether analogue of DOPC. These results suggest that the depth dependence of Glu ionization in lipid-bilayer membranes may be steeper than previously predicted or envisioned.

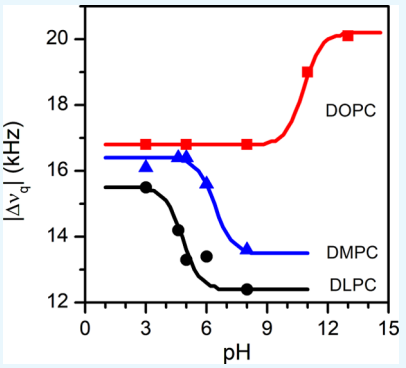

INTRODUCTION

A lipid-bilayer membrane consists of a low dielectric hydrophobic interior flanked by polar lipid head groups and buffered aqueous phases that constitute the high dielectric content of the outer and inner cellular spaces. While the membrane interior would appear to be inhospitable to charged functional groups, membrane proteins nevertheless sometimes contain titratable residues within this region. The presence of charged groups furthermore is important for the biological functions of numerous membrane proteins. The side-chain protonation states of residues such as His, Lys, Arg, Glu, and Asp are dependent on numerous local electrostatic environmental factors such as lipid hydrophobic effects, hydrogen bonding, membrane fluidity, and solvent accessibility.[1−4] The charged state of such residues will then have consequences for the folding, orientation, and dynamics of secondary-structure elements in membrane proteins. Arg residues, for example, are found throughout the voltage-sensing domains of various channel proteins[5,6] and have been observed to cause helix reorientations[7] and helix distortions even within individual model peptides.[8] Glu can be found in the interior of certain membrane proteins and, when charged, can alter protein folding.[9] Furthermore, Glu is critical for proton pumping in crucial systems such as bacteriorhodopsin[10,11] and cytochrome c oxidase.[12−14] For directional proton translocations and other functions, the local environment and the local ionization constants for particular Glu residues will be significant. To this end, we investigate the ionization properties of a well-defined Glu residue held on a model helix in lipid-bilayer membranes of different thicknesses. Indeed, computational predictions have indicated that the side chain Glu pK_a should change with the bilayer thickness.[15]

Selectively deuterated model transmembrane helical peptides have been proven to be useful for the measurement of side-chain ionization behavior. Solid-state NMR spectra of oriented samples of such membrane helices can be analyzed to reveal the helix tilt in each membrane as a function of pH. Changes in the spectra may then reveal the titration point for a helix reorientation. In our designed framework, only one ionizable group is present on the helix. The titration behavior can then reflect the pK_a of the individual defined residue at various depths within lipid-bilayer membranes. The model GW[5,19]ALP23 sequence (acetyl-GGALW(LA)$_6$LWLAGA-amide) is useful for this approach because its helix adopts a

Received: January 15, 2021
Accepted: March 8, 2021
Published: March 17, 2021

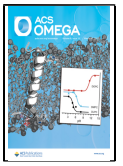

well-defined tilt within lipid bilayers. Indeed, $GW^{5,19}$ALP23 has been employed for the measurement of the pK_a values of individual Lys, His, and Arg residues.[16−18] Experiments with Glu residues have proven more difficult. Varying degrees of success have been achieved while characterizing the protonation state of Glu, made difficult by a rather indifferent response of the helix to the ionization state of the carboxylate side chain.[19]

In this article, we probe the titration point of the Glu side chain near the membrane interface of 1,2-dilauroyl-*sn*-glycero-3-phosphocholine (DLPC), 1,2-dimyristoyl-*sn*-glycero-3-phosphatidylcholine (DMPC), and 1,2-dioleoyl-*sn*-glycero-3-phosphocholine (DOPC) bilayers, again using the $GW^{5,19}$ALP23 sequence. Residue L4 of the parent sequence was mutated to Glu (Table 1 and Figure 1). As expected, the tilt of the core helix was greatly altered by the L4 to E4 mutation. The pK_a of the E4 Glu side chain was then determined by observing pH-dependent changes in ^{2}H NMR spectra, from oriented bilayer membrane samples, that reported the neighboring alanine A3 deuterated methyl group quadrupolar splitting. Residue A3 proved to be an effective sensor of the pH response even though the tilt of the central membrane-spanning helix changed very little with pH. Titration points determined in DLPC, DMPC, and DOPC bilayers show a surprisingly dramatic dependence on the bilayer thickness despite the interfacial location of the Glu residue. The results are important for understanding key aspects for the regulation of membrane protein function.

Table 1. Sequences of Peptides[a]

name	sequence	reference
$GW^{5,19}$ALP23	acetyl-GGALW^{5}LALALALALALALW^{19}LAGA-amide	37
$E^4GW^{5,19}$ALP23	acetyl-GGAEW^{5}LALALALALALALW^{19}LAGA-amide	this work
$E^4A^5GW^{19}$ALP23	acetyl-GGAEA^{5}LALALALALALALW^{19}LAGA-amide	this work

[a]Selected alanine residues were deuterated; see the Materials and Methods section.

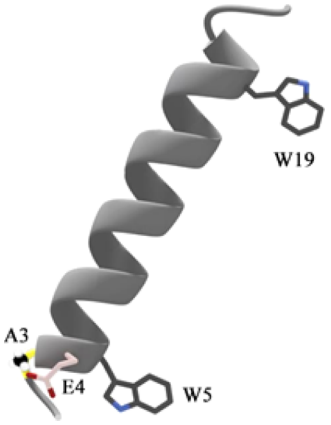

Figure 1. Tilted model of the helix of $E^4GW^{5,19}$ALP23 in a bilayer membrane, highlighting the side chains of residues A3, E4, W5, and W19.

RESULTS

We monitored the ^{2}H quadrupolar splitting of labeled alanine A3 in $E^4GW^{5,19}$ALP23 as a function of pH. The C_β methyl ^{2}H quadrupolar splitting of residue A3 decreases from 15.5 to 12.4 kHz in DLPC bilayers and from 16.1 to 13.6 kHz in DMPC within the pH range of 3.0−8.0, and increases from 16.8 kHz in DOPC up to 20.1 kHz in the ether-linked analogue of DOPC when the pH range is 8.0−13.0 (Table 2 and Figure 2). Because the sequence contains no other ionizable residues, these observed changes in the NMR spectra are directly related to the charged state of the glutamic acid E4 side chain. The use of the ether analogue of DOPC at a high pH does not alter the helix properties.[17,18]

In contrast to alanine A3, the ^{2}H NMR spectra of labeled alanines in the core helix of $E^4GW^{5,19}$ALP23 do not change with pH (Figure 3). Whether the peptide is in bilayers of DOPC, DMPC, or DLPC, the quadrupolar splittings for the core alanines and therefore the orientation of the core helix with respect to the bilayer normal remain essentially unchanged from pH 3 to 8. The changes for alanine A3, though modest, show defined trends with pH, indicating that the deviation of A3 from the core helix responds to pH. We attribute the pH dependence to the titration of glutamic acid E4. Because residues A3 and E4 are outside of the core helix, it is understandable that the relative fraying reported by A3 could change while the core helix remains unaffected by the ionization change at residue E4.

To further assess the core helix and the influence of tryptophan W5, adjacent to the ionizable E4, W5 was mutated to Ala and labeled as Ala-CD_3. Once again, no difference in the A5 quadrupolar splitting was observed over the pH range of 3.0−8.0 in DLPC bilayers (Figure 3B). These results confirm that the core transmembrane helix extends back to residue 5 and is insensitive to the ionization state of the E4 side chain.

Returning now to the A3 methyl group on the unwound portion of the helix, the pH dependence of the ^{2}H quadrupolar splitting reveals titration midpoints in bilayers of DLPC, DMPC, and DOPC (Figure 4). The midpoints and thereby the predicted pK_a values for the glutamic acid E4 side chain show a remarkable lipid dependence, namely, 4.8 in DLPC, 6.3 in DMPC, and 11.0 in DOPC (Figure 4). As noted, the use of the ether analogue of DOPC at high pH does not affect the helix properties.[17,18]

The mere presence of glutamic acid E4 greatly influences the helix tilt (Figure 5). In DLPC bilayers, the mean tilt of the core helix from the bilayer normal decreases from 20° with L4 to about 5° with E4 (Table 3). When the pH is increased from 3 to 8 in DLPC, the helix orientation does not change, but alanine A7 no longer resides within the core helix at pH 8 (Figure 5, top), reflecting a more extensive unraveling of the core helix at pH 8. The deviation of alanine A3 from the core helix changes both when E4 is introduced and when the pH is increased, reflecting the titration of E4.

In DMPC, residue 7 stays within the core helix, whose orientation again does not depend on the pH (Figure 5, middle). Notably, with E4 present, the core helix orientation is essentially the same in DMPC and DLPC (Table 3). The core helix tilt is much less with E4 than with L4. Indeed, the slight tilt of the core helix of $E^4GW^{5,19}$ALP23 in DLPC or DMPC is about the minimum value (~4°) consistent with cone precession.[20] The mean helix azimuthal rotation ρ_0 changes in both lipids by about 30°, probably reflecting optimal access

https://doi.org/10.1021/acsomega.1c00276
ACS Omega 2021, 6, 8488−8494

Table 2. Quadrupolar Splitting Magnitudes ($|\Delta\nu_q|$, in kHz) for Labeled Alanine CD_3 Groups of $GW^{5,19}$ALP23 with Glu-4 or Leu-4 in Oriented Bilayer Membranes[a]

			Ala-CD_3 quadrupolar splittings in kHz[a]							
residue 4	lipid	pH	A3	A7	A9	A11	A13	A15	A17	ref
Leu	DLPC	–[b]	27.5	26.4	25.5	26.9	14.6	20.7	3.4	37 and 38
Glu	DLPC	3	15.5	11.0	0.6	12.4	0.5	11.0	–[c]	this work
Glu	DLPC	5	13.3	–[c]	–[c]	–[c]	–[c]	–[c]	–[c]	this work
Glu	DLPC	8	12.4	18.7	2.4	11.9	1.7	–[c]	–[c]	this work
Leu	DMPC	–[b]	10.8	21.9	8.9	20.9	3.8	17.6	2.9	37 and 38
Glu	DMPC	3	16.1	10.3	2.1	11.5	1.1	10.2	4.2	this work
Glu	DMPC	5	16.4	–[c]	–[c]	–[c]	–[c]	–[c]	–[c]	this work
Glu	DMPC	8	13.6	9.9	3.6	11.2	1.5	11.2	2.8	this work
Leu	DOPC	–[b]	10.4	16.6	1.7	16.7	1.5	15.4	2.6	37 and 38
Glu	DOPC	3	16.8	8.4	6.5	9.8	3.6	11.8	2.8	this work
Glu	DOPC	5	16.8	–[c]	–[c]	–[c]	–[c]	–[c]	–[c]	this work
Glu	DOPC	8	16.8	8.9	6.3	–[c]	–[c]	–[c]	–[c]	this work
Glu	DOPC	11	19.0	9.2	5.6	–[c]	–[c]	–[c]	–[c]	this work

[a]Values are reported in kHz for a $\beta = 0°$ sample orientation. The experimental uncertainty is about ±1 kHz. [b]Unbuffered at neutral pH. The peptide helix with leucine L4 has no ionizable groups and shows no pH dependence. [c]Values not listed were not measured.

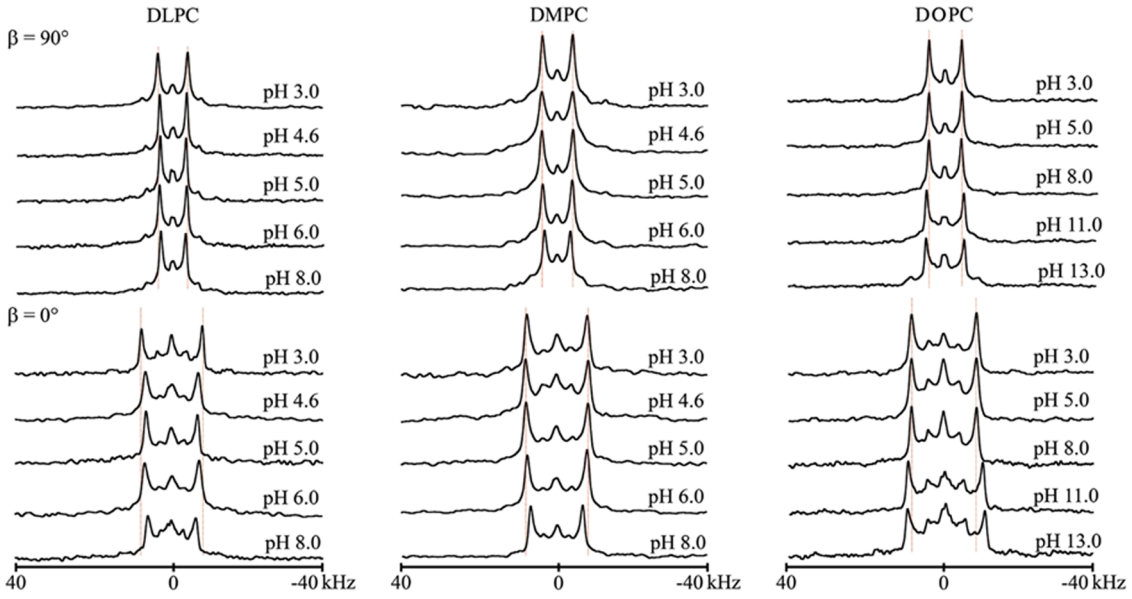

Figure 2. ^{2}H NMR spectra for labeled alanine A3 of $E^4GW^{5,19}$ALP23 in mechanically aligned bilayers of DLPC, DMPC, and DOPC, oriented at β = 90 and 0°, temperature 50 °C, and sample pH as indicated. For experiments above pH 8, the membrane was made from the ether-linked analogue of DOPC.

of the E4 side chain to the aqueous interface. Conspicuously, the rotational slippage $\sigma\rho$ in each membrane decreases from a moderate value of about 40° with L4 down to a very low value of about 5° with E4 (Table 3), suggesting a well-defined helix orientation when E4 is present. Importantly, the GALA and Gaussian analyses predict the same orientations for the core helix, dictated by τ_0 and ρ_0.

Likewise, in DOPC, the orientation of the core helix remains low and insensitive to pH. Regardless of whether the pH is 3 or 8 (Figure 5, bottom), the ^{2}H Ala quadrupolar splittings remain unchanged. Within the context of the low helix tilt (Table 3), alanine A7 remains part of the core helix in DOPC as well as in DMPC, even though A7 deviates from the core helix in DLPC at high pH (Figure 5). In DOPC, alanine A3 shows a pH dependence (Figure 5) for its deviation from the core helix, with a midpoint near pH 11 (Figure 4). The fits for the core helix properties by the GALA and Gaussian analyses again agree in DOPC (Table 3).

DISCUSSION

Previous measurements and estimates of the Glu pK_a in lipid environments have revealed values higher than the aqueous value, as expected, but have been largely silent with respect to lipid dependence. Notably, MacCallum et al.[15] predicted explicitly that the pK_a would depend upon the depth of insertion of a Glu residue into a lipid bilayer. Experimentally, in bovine cytochrome *c* oxidase, buried Glu 242, which is critical for proton pumping, has been assigned a pK_a of about 12.[13,21] Similarly, in bacteriorhodopsin, buried Glu 204, also critical for proton pumping, has been assigned a high pK_a value between 9 and 12.[11,22−24] Likewise, a pK_a of about 8.7 has been measured for a buried Asp residue in a model transmembrane helix formed by the peptide

https://doi.org/10.1021/acsomega.1c00276
ACS Omega 2021, 6, 8488−8494

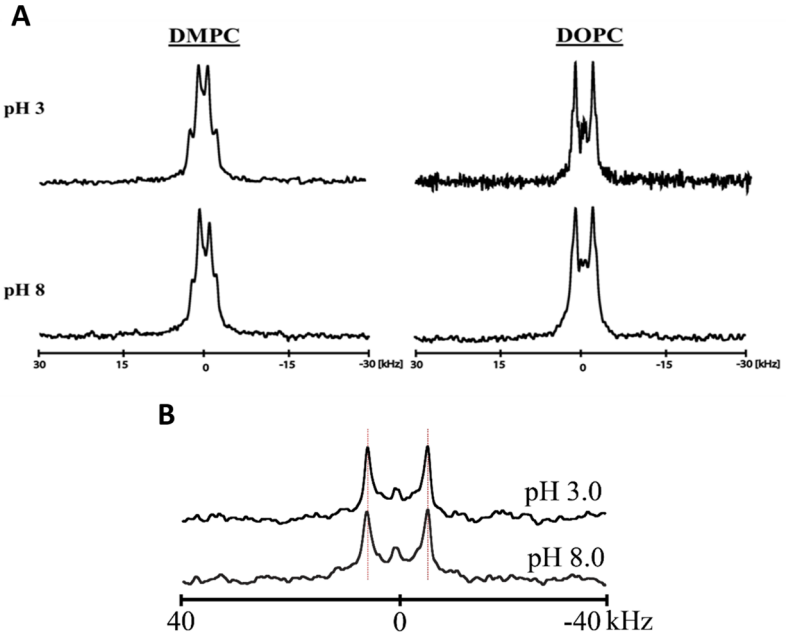

Figure 3. (A) ^{2}H NMR spectra for deuterated core alanines A7 (50% ^{2}H) and A9 (100% ^{2}H) in E^{4}GW^{5,19}ALP23 in DMPC or DOPC lipid bilayers at pH 3 and 8. (B) ^{2}H NMR spectra for deuterated alanine A5 of E^{4}A^{5}GW^{19}ALP23 in DLPC bilayers at pH 3 and 8. Each sample is oriented at β = 90°, and the temperature is 50 °C.

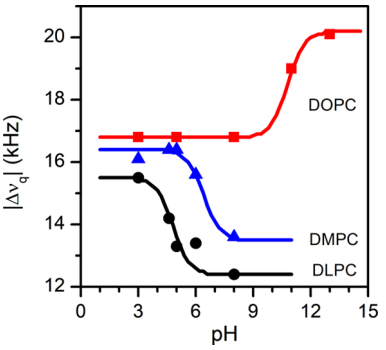

Figure 4. Titration curves monitoring the side-chain CD_3 quadrupolar splitting of alanine A3 in E^{4}GW^{5,19}ALP23 within oriented bilayers of DLPC (black), DMPC (blue), and DOPC (red). The midpoints of the curves indicate pK_a values of 4.8 (DLPC), 6.3 (DMPC), and 11.0 (DOPC).

KKGL$_7$DLWL$_9$KKA.[3] An earlier study with E14 or E16 in the present framework of GWALP23[19] suggested high pK_a values, yet little dependence on the lipid membrane thickness and little response of a transmembrane core helix to Glu ionization. A high pK_a of about 9.8, furthermore, has been predicted computationally for the Glu residue of E^{14}GWALP23.[25] Nevertheless, in spite of the consistent pattern that has emerged among the numerous examples, a predicted lipid dependence[15] for the Glu pK_a in a transmembrane helix has remained essentially untested or undetected.

The present work addresses glutamic acid E4 in the transmembrane framework of GWALP23. This Glu substitution is situated relatively near a membrane interface, notably less buried than the examples noted above. Indeed, one could expect perhaps little or no connection between the preferred Glu ionization state and the thickness of a host lipid membrane for the E^{4}GWALP23 helix. Nonetheless, our results reveal a remarkable lipid dependence for the E4 ionization. The pH dependence can be assigned reliably to residue E4 because previous studies have confirmed that no titration is observed for the parent peptide framework, as no ionizable residues are included within the sequence,[17] prior to the introduction of E4. Each of the lipid membranes, DLPC, DMPC, and DOPC, was investigated above the lipid phase transition temperature, importantly in the physiologically relevant liquid-crystalline bilayer phase. Because gel-phase conditions were not investigated, the lipid phase is not a factor for the Glu titrations reported here. Acyl chain unsaturation also is unlikely to be a significant factor for the titration behavior, as related experiments have shown that chain unsaturation is relatively unimportant for the lipid interactions or orientations of helices with charged residues.[26] By contrast, bilayer thickness is highly important for regulating the orientations of Arg-containing helices.[26]

The results for titrating glutamic acid E4 reveal a pK_a (4.8) close to the aqueous value at the DLPC membrane interface (Figure 4) and higher values of 6.3 and 11, respectively, in DMPC and DOPC. Notably, the tilt of the E4-containing core helix does not change with the pH in any of the membranes that were examined, in agreement with earlier results for helices with more buried Glu residues.[19] The results are significant because they indicate that the aqueous access of membrane protein functional groups is variable even at locations within or near a membrane interface. Indeed, the pH dependence can reflect changes in helix unraveling, as noted here, as well as changes in helix orientation, as noted previously for Lys residue titration.[16] Small perturbations therefore will be able to influence ionization states and membrane protein function. For example, a key glutamic acid residue E120 in the pH "gate" of the KcsA potassium channel is near a membrane interface and has a pK_a that varies with the K^+ concentration.[27] When measured in 1,2-dioleoyl-*sn*-glycero-3-phosphoethanolamine (DOPE)/1,2-dioleoyl-*sn*-glycero-3-phosphoserine (DOPS) at pH 7.5, this residue, E120, is protonated at 50 μM [K^+], yet deprotonated at 80 mM [K^+].[27] These results with the KcsA channel suggest a situation similar

https://doi.org/10.1021/acsomega.1c00276
ACS Omega 2021, 6, 8488−8494

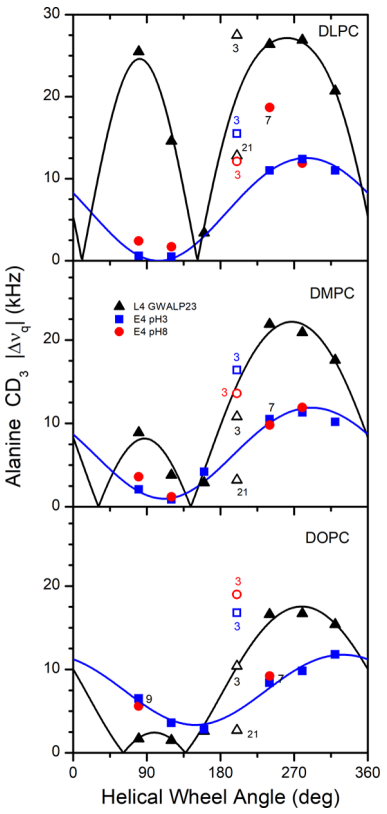

Figure 5. GALA wave plots to compare the core helix orientations for GWALP23 when E4 or L4 is present. Quadrupolar wave plots are presented for the helices in DLPC, DMPC, and DOPC, as indicated. In each membrane, the core helix tilt changes when L4 (black curves) is changed to E4 but does respond to the ionization of E4 (blue and red data points). When E4 titrates in DLPC, the extent of the unraveling of residue 3 changes, and residue 7 also becomes unwound from the core helix. When E4 titrates in DMPC or DOPC, residue 3 again responds, but residue 7 remains on the curve for the core helix. In DOPC, residue 3 is on the curve for the parent core helix with L4 but unravels when E4 is introduced and deviates still further when E4 titrates.

to the present one, where subtle factors influence the pK_a of an interfacial Glu residue. The high pK_a observed for residue E4 of our model helix in DOPC furthermore offers support for previous experiments that suggested high titration points for more deeply buried Glu side chains in DLPC as well as DOPC.[19] Indeed, the present new observations for the increase in the E4 pK_a with bilayer thickness illustrate a lipid dependence for an interfacial residue that was not observed for more buried residues. When a charged group is near a bilayer interface, additional factors including water penetration and bilayer deformation have been shown computationally to make important contributions to the lipid−protein interactions.[7,28] The diverse array of molecular interactions leads to a complex and still puzzling picture of the membrane interface.

In conclusion, glutamic acid E4 resides outside of the transmembrane helix of acetyl-GGALW(LA)$_6$LWLAGA-amide, yet is adjacent to the core helix at a bilayer membrane interface. The extent of helix unraveling is reported by deuterated alanine A3 when E4 titrates. The ionization behavior of residue E4 is remarkably lipid dependent, showing pK_a values of 4.8, 6.3, and 11, respectively, in DLPC, DMPC, and DOPC bilayers. The results suggest that subtle regulatory changes near cell membrane interfaces are likely to influence ionization states, molecular signaling, and membrane protein function.

MATERIALS AND METHODS

Labeled samples of the peptide E^{4}GW^{5,19}ALP23 or E^{4}A^{5}GW^{5,19}ALP23 (Table 1) were synthesized with specifically placed ^{2}H-alanines as described previously.[29−31] Briefly, fluorenylmethoxycarbonyl (Fmoc)-amino acids were purchased from NovaBiochem (San Diego, CA). Commercial L-Ala-d_4 was purchased from Cambridge Isotope Labs (Andover, MA) and was modified with an Fmoc group as described.[17] Peptide synthesis was achieved via solid-phase FastMoc chemistry on a 0.1 mmol scale.[32,33] Ala-d_4 was incorporated either at alanine A3 (100%) or on two of the core helix alanines at 100 and 50% respective ^{2}H label abundance. Peptides were purified via reversed-phase high-performance liquid chromatography (HPLC) on an octyl silica column (Zorbax Rx-C8, 9.4 × 250 mm^2, 5 μm particle size; Agilent Technologies, Santa Clara, CA) using a gradient of 92−98% methanol (with 0.1% trifluoroacetic acid) over 40 min. The chromatographic purification effectively removed traces of incompletely synthesized shorter peptides as well as any residual traces of trifluoroacetic acid. The peptide mass and purity are confirmed in Figure S1 of the Supporting Information.

Solid-state NMR experiments were performed using mechanically aligned peptide−lipid samples (1:60 mol/mol) prepared as described[29,33] using DLPC, DMPC, and DOPC lipids purchased from Avanti Polar Lipids (Alabaster, AL). For experiments above pH 8, the alkali-stable ether-linked analogue of DOPC was employed. Peptide/lipid films were deposited on

Table 3. Geometric Analysis of Labeled Alanines (GALA) and Gaussian Analyses of Helix Orientations and Dynamics Using Ala-CD$_3$ $|\Delta\nu_q|$ Magnitudes[a]

		GALA				Gaussian[a]					
lipid	peptide	τ_0 (deg)	ρ_0 (deg)	S_{zz}	RMSD	τ_0 (deg)	ρ_0 (deg)	$\sigma\rho$ (deg)	$\sigma\tau$ (deg)	RMSD	ref
DLPC	GWALP23	21	305	0.71	0.7	23	304	33	5[b]	0.7	31
	E^4 GWALP23[c]	4	328	0.7	0.3	4	334	16	5[b]	1.4	this work
DMPC	GWALP23	9	311	0.88	1.0	13	308	44	5[b]	1.1	33
	E^4 GWALP23	4	325	0.7	0.3	3	333	4	5[b]	1.3	this work
DOPC	GWALP23	6	323	0.87	0.6	9	321	48	5[b]	0.7	31
	E^4 GWALP23	3	373	0.82	0.5	3	375	24	5[b]	0.6	this work

[a]The modified Gaussian analysis followed Sparks et al.,[31] with S_{zz} fixed at 0.88 and $\sigma\tau$ fixed at 5°. [b]Fixed value. [c]The tilt of the core helix of E^{4}GWALP23 is observed not to change with pH (see Figure 5). The helix of GWALP23 has no ionizable residues, so its tilt also does not change with pH.

https://doi.org/10.1021/acsomega.1c00276
ACS Omega 2021, 6, 8488−8494

thin glass slides from 95% methanol, dried under vacuum (10^{-4} Torr for 48 h), and hydrated (45% w/w) with deuterium-depleted water (Cambridge Isotope Laboratories, Andover, MA) containing 20 mM glycine, citrate, or tris buffer at a specific pH value between 3 and 13.[17,18] The hydrated slides were stacked in 8 mm cuvettes, sealed with epoxy, and incubated at 40 °C for at least 48 h to enable bilayer alignment. Bilayer alignment was confirmed by ^{31}P NMR at 121.5 MHz using a 300 MHz (7.05 T) Bruker Avance Spectrometer with broad-band ^{1}H decoupling (4.2 kHz); see Figure S2 of the Supporting Information. Deuterium (^{2}H) NMR experiments were performed at 46 MHz using a 300 MHz Bruker Avance Spectrometer with a solid quadrupolar-echo pulse sequence[34] with a 3.0 μs 90° pulse length, a 90 ms recycle delay, and a 115 μs echo delay. The spectra were recorded using 0.9−1.4 million scans and were processed with 100 Hz line broadening.

The tilt of the core helix and, importantly, the deviation of alanine A3 from the core helix were estimated from the ^{2}H Ala quadrupolar splittings using a semistatic "geometric analysis of labeled alanines" ("GALA") method.[8,29] Residue A3 was not included in the calculation of the mean helix tilt. The results for the helix orientation were confirmed by an independent modified Gaussian analysis.[31,35] Figure 1 was drawn using PyMol,[36] licensed from Schrödinger, Inc. (Portland, OR). In principle, either the tilt of the core helix, the rotation of the core helix, or the deviation of A3 from the core helix could show a pH dependence. The side chain of E4 is the only titratable group in the E^{4}GW^{5,19}ALP23 peptide (Table 1).

■ ASSOCIATED CONTENT

Supporting Information

The Supporting Information is available free of charge at https://pubs.acs.org/doi/10.1021/acsomega.1c00276.

Mass spectra, HPLC chromatograms; and ^{31}P NMR spectra (PDF)

■ AUTHOR INFORMATION

Corresponding Author

Roger E. Koeppe, II − *Department of Chemistry and Biochemistry, University of Arkansas, Fayetteville, Arkansas 72701, United States;* orcid.org/0000-0003-0676-6413; Email: rk2@uark.edu

Authors

Matthew J. McKay − *Department of Chemistry and Biochemistry, University of Arkansas, Fayetteville, Arkansas 72701, United States*

Kelsey A. Marr − *Department of Chemistry and Biochemistry, University of Arkansas, Fayetteville, Arkansas 72701, United States*

Jake R. Price − *Department of Chemistry and Biochemistry, University of Arkansas, Fayetteville, Arkansas 72701, United States*

Denise V. Greathouse − *Department of Chemistry and Biochemistry, University of Arkansas, Fayetteville, Arkansas 72701, United States;* orcid.org/0000-0001-7104-8499

Complete contact information is available at: https://pubs.acs.org/10.1021/acsomega.1c00276

Author Contributions

This manuscript was written through contributions of all authors. All authors have given approval to the final version of the manuscript.

Funding

US National Science Foundation grant MCB 1713242. Arkansas Biosciences Institute.

Notes

The authors declare no competing financial interest.

■ ACKNOWLEDGMENTS

With heartfelt thanks, we dedicate this paper to the late Prof. James F. Hinton, to whom we are indebted for numerous vital discussions.

■ ABBREVIATIONS

DLPC, 1,2-dilauroyl-*sn*-glycero-3-phosphocholine; DMPC, 1,2-dimyristoyl-*sn*-glycero-3-phosphocholine; DOPC, 1,2-dioleoyl-*sn*-glycero-3-phosphocholine; DOPE, 1,2-dioleoyl-*sn*-glycero-3-phosphoethanolamine; DOPS, 1,2-dioleoyl-*sn*-glycero-3-phosphoserine; Fmoc, fluorenylmethoxycarbonyl; GALA, geometric analysis of labeled alanines; GWALP23, acetyl-GGALW(LA)$_6$LWLAGA-amide; RMSD, root-mean-square deviation

■ REFERENCES

(1) Kuhlman, B.; Luisi, D. L.; Young, P.; Raleigh, D. P. pK(a) Values and the pH Dependent Stability of the N-terminal Domain of L9 as Probes of Electrostatic Interactions in the Denatured State. Differentiation between Local and Nonlocal Interactions. *Biochemistry* **1999**, *38*, 4896−4903.

(2) Forsyth, W. R.; Antosiewicz, J. M.; Robertson, A. D. Empirical Relationships between Protein Structure and Carboxyl pK(a) Values in Proteins. *Proteins* **2002**, *48*, 388−403.

(3) Caputo, G. A.; London, E. Position and Ionization State of Asp in the Core of Membrane-Inserted Alpha Helices Control Both the Equilibrium between Transmembrane and Nontransmembrane Helix Topography and Transmembrane Helix Positioning. *Biochemistry* **2004**, *43*, 8794−8806.

(4) Silva, A. M. N.; Kong, X. L.; Hider, R. C. Determination of the pKa Value of the Hydroxyl Group in the Alpha-Hydroxycarboxylates Citrate, Malate and Lactate by ^{13}C NMR: Implications for Metal Coordination in Biological Systems. *BioMetals* **2009**, *22*, 771−778.

(5) Clayton, G. M.; Altieri, S.; Heginbotham, L.; Unger, V. M.; Morais-Cabral, J. H. Structure of the Transmembrane Regions of a Bacterial Cyclic Nucleotide-Regulated Channel. *Proc. Natl. Acad. Sci. U.S.A.* **2008**, *105*, 1511−1515.

(6) Schwaiger, C. S.; Bjelkmar, P.; Hess, B.; Lindahl, E. 3(10)-Helix Conformation Facilitates the Transition of a Voltage Sensor S4 Segment toward the Down State. *Biophys. J.* **2011**, *100*, 1446−1454.

(7) Vostrikov, V. V.; Hall, B. A.; Greathouse, D. V.; Koeppe, R. E., 2nd; Sansom, M. S. Changes in Transmembrane Helix Alignment by Arginine Residues Revealed by Solid-State NMR Experiments and Coarse-Grained Md Simulations. *J. Am. Chem. Soc.* **2010**, *132*, 5803−5811.

(8) McKay, M. J.; Fu, R.; Greathouse, D. V.; Koeppe, R. E., II Breaking the Backbone: Central Arginine Residues Induce Membrane Exit and Helix Distortions within a Dynamic Membrane Peptide. *J. Phys. Chem. B* **2019**, *123*, 8034−8047.

(9) Achilonu, I.; Fanucchi, S.; Cross, M.; Fernandes, M.; Dirr, H. W. Role of Individual Histidines in the pH-Dependent Global Stability of Human Chloride Intracellular Channel 1. *Biochemistry* **2012**, *51*, 995−1004.

(10) Dioumaev, A. K.; Richter, H. T.; Brown, L. S.; Tanio, M.; Tuzi, S.; Saito, H.; Kimura, Y.; Needleman, R.; Lanyi, J. K. Existence of a Proton Transfer Chain in Bacteriorhodopsin: Participation of Glu-194

in the Release of Protons to the Extracellular Surface. *Biochemistry* **1998**, *37*, 2496−2506.
(11) Freier, E.; Wolf, S.; Gerwert, K. Proton Transfer Via a Transient Linear Water-Molecule Chain in a Membrane Protein. *Proc. Natl. Acad. Sci. U.S.A.* **2011**, *108*, 11435−11439.
(12) Wikstrom, M.; Ribacka, C.; Molin, M.; Laakkonen, L.; Verkhovsky, M.; Puustinen, A. Gating of Proton and Water Transfer in the Respiratory Enzyme Cytochrome C Oxidase. *Proc. Natl. Acad. Sci. U.S.A.* **2005**, *102*, 10478−10481.
(13) Popović, D. M.; Quenneville, J.; Stuchebrukhov, A. A. DFT/Electrostatic Calculations of pK(a) Values in Cytochrome C Oxidase. *J. Phys. Chem. B* **2005**, *109*, 3616−3626.
(14) Lu, J. X.; Gunner, M. R. Characterizing the Proton Loading Site in Cytochrome C Oxidase. *Proc. Natl. Acad. Sci. U.S.A.* **2014**, *111*, 12414−12419.
(15) MacCallum, J. L.; Bennett, W. F.; Tieleman, D. P. Distribution of Amino Acids in a Lipid Bilayer from Computer Simulations. *Biophys. J.* **2008**, *94*, 3393−3404.
(16) Gleason, N. J.; Vostrikov, V. V.; Greathouse, D. V.; Koeppe, R. E., 2nd Buried Lysine, but Not Arginine, Titrates and Alters Transmembrane Helix Tilt. *Proc. Natl. Acad. Sci. U.S.A.* **2013**, *110*, 1692−1695.
(17) Martfeld, A. N.; Greathouse, D. V.; Koeppe, R. E., 2nd Ionization Properties of Histidine Residues in the Lipid Bilayer Membrane Environment. *J. Biol. Chem.* **2016**, *291*, 19146−19156.
(18) Thibado, J. K.; Martfeld, A. N.; Greathouse, D. V.; Koeppe, R. E., II Influence of High pH and Cholesterol on Single Arginine-Containing Transmembrane Peptide Helices. *Biochemistry* **2016**, *55*, 6337−6343.
(19) Rajagopalan, V.; Greathouse, D. V.; Koeppe, R. E., 2nd Influence of Glutamic Acid Residues and pH on the Properties of Transmembrane Helices. *Biochim. Biophys. Acta, Biomembr.* **2017**, *1859*, 484−492.
(20) Lee, J.; Im, W. Transmembrane Helix Tilting: Insights from Calculating the Potential of Mean Force. *Phys. Rev. Lett.* **2008**, *100*, No. 018103.
(21) Wikström, M.; Jasaitis, A.; Backgren, C.; Puustinen, A.; Verkhovsky, M. I. The Role of the D- and K-pathways of Proton Transfer in the Function of the Haem-Copper Oxidases. *Biochim. Biophys. Acta, Bioenerg.* **2000**, *1459*, 514−520.
(22) Richter, H. T.; Brown, L. S.; Needleman, R.; Lanyi, J. K. A Linkage of the pK(a)'S of Asp-85 and Glu-204 Forms Part of the Reprotonation Switch of Bacteriorhodopsin. *Biochemistry* **1996**, *35*, 4054−4062.
(23) Sampogna, R. V.; Honig, B. Electrostatic Coupling between Retinal Isomerization and the Ionization State of Glu-204: A General Mechanism for Proton Release in Bacteriorhodopsin. *Biophys. J.* **1996**, *71*, 1165−1171.
(24) Morgan, J. E.; Vakkasoglu, A. S.; Lanyi, J. K.; Lugtenburg, J.; Gennis, R. B.; Maeda, A. Structure Changes Upon Deprotonation of the-Proton Release Group in the Bacteriorhodopsin Photocycle. *Biophys. J.* **2012**, *103*, 444−452.
(25) Panahi, A.; Brooks, C. L. Membrane Environment Modulates the pK(a) Values of Transmembrane Helices. *J. Phys. Chem. B* **2015**, *119*, 4601−4607.
(26) Lipinski, K.; McKay, M. J.; Afrose, F.; Martfeld, A. N.; Koeppe, R. E., 2nd; Greathouse, D. V. Influence of Lipid Saturation, Hydrophobic Length and Cholesterol on Double-Arginine-Containing Helical Peptides in Bilayer Membranes. *ChemBioChem* **2019**, *20*, 2784−2792.
(27) Sun, Z. Y.; Xu, Y. Y.; Zhang, D. Y.; McDermott, A. E. Probing Allosteric Coupling in a Constitutively Open Mutant of the Ion Channel KcsA Using Solid-State NMR. *Proc. Natl. Acad. Sci., U.S.A.* **2020**, *117*, 7171−7175.
(28) Vorobyov, I.; Olson, T. E.; Kim, J. H.; Koeppe, R. E., 2nd; Andersen, O. S.; Allen, T. W. Ion-Induced Defect Permeation of Lipid Membranes. *Biophys. J.* **2014**, *106*, 586−597.
(29) van der Wel, P. C.; Strandberg, E.; Killian, J. A.; Koeppe, R. E., 2nd Geometry and Intrinsic Tilt of a Tryptophan-Anchored Transmembrane Alpha-Helix Determined by ^{2}H NMR. *Biophys. J.* **2002**, *83*, 1479−1488.
(30) Gleason, N. J.; Vostrikov, V. V.; Greathouse, D. V.; Grant, C. V.; Opella, S. J.; Koeppe, R. E., 2nd Tyrosine Replacing Tryptophan as an Anchor in GWALP Peptides. *Biochemistry* **2012**, *51*, 2044−2053.
(31) Sparks, K. A.; Gleason, N. J.; Gist, R.; Langston, R.; Greathouse, D. V.; Koeppe, R. E., 2nd Comparisons of Interfacial Phe, Tyr, and Trp Residues as Determinants of Orientation and Dynamics for GWALP Transmembrane Peptides. *Biochemistry* **2014**, *53*, 3637−3645.
(32) Greathouse, D. V.; Koeppe, R. E., II; Providence, L. L.; Shobana, S.; Andersen, O. S. Design and Characterization of Gramicidin Channels. *Methods Enzymol.* **1999**, *294*, 525−550.
(33) McKay, M. J.; Martfeld, A. N.; De Angelis, A. A.; Opella, S. J.; Greathouse, D. V.; Koeppe, R. E., II Control of Transmembrane Helix Dynamics by Interfacial Tryptophan Residues. *Biophys. J.* **2018**, *114*, 2617−2629.
(34) Davis, J. H.; Jeffrey, K. R.; Valic, M. I.; Bloom, M.; Higgs, T. P. Quadrupolar Echo Deuteron Magnetic Resonance Spectroscopy in Ordered Hydrocarbon Chains. *Chem. Phys. Lett.* **1976**, 390−394.
(35) Strandberg, E.; Esteban-Martin, S.; Ulrich, A. S.; Salgado, J. Hydrophobic Mismatch of Mobile Transmembrane Helices: Merging Theory and Experiments. *Biochim. Biophys. Acta, Biomembr.* **2012**, *1818*, 1242−1249.
(36) DeLano, W. L. *The PyMOL Molecular Graphics System*; Delano Scientific: San Carlos, CA, 2002.
(37) Vostrikov, V. V.; Daily, A. E.; Greathouse, D. V.; Koeppe, R. E., 2nd Charged or Aromatic Anchor Residue Dependence of Transmembrane Peptide Tilt. *J. Biol. Chem.* **2010**, *285*, 31723−31730.
(38) Afrose, F.; McKay, M. J.; Mortazavi, A.; Suresh Kumar, V.; Greathouse, D. V.; Koeppe, R. E., 2nd Transmembrane Helix Integrity Versus Fraying to Expose Hydrogen Bonds at a Membrane-Water Interface. *Biochemistry* **2019**, *58*, 633−645.

https://doi.org/10.1021/acsomega.1c00276
ACS Omega 2021, 6, 8488−8494